Phys. Status Solidi A **213,** No. 2, 384–389 (2016) / **DOI** 10.1002/pssa.201532579

Part of Topical Section on
Magnetism and Applications of Magnetic Wires

physica status solidi a
www.pss-a.com
applications and materials science

Directed crystallization of glass-coated microwires

V. Larin[1], L. V. Panina[*,2], E.-A. Patroi[3], D. Patroi[3], V. Bashev[4], and N. Kutseva[4]

[1] MFTI Ltd., Kishinev, Moldova
[2] National University of Science and Technology, MISiS, Moscow, Russia
[3] ICPE SA, Bucharest, Romania
[4] UNU, Dnepropetrovsk, Ukraine

Received 31 July 2015, revised 19 January 2016, accepted 19 January 2016
Published online 3 February 2016

Keywords coercivity, directed crystallization, glass-coated microwire, micro magnet

[*] Corresponding author: e-mail lpanina@plymouth.ac.uk, Phone: +79152563580

In this work, the directed crystallization of glass-coated magnetic microwires of Co-rich composition is realized with the aim to develop a novel technique for micro-magnet fabrication. The onset of the process is caused by local overheating above the primary crystallization temperature while the rest of the wire sample is at the temperature slightly below the crystallization temperature. This creates the conditions for spontaneous formation of microcrystallites at the wire edge and the movement of the crystal–amorphous interface along the wire. It was found that the directed crystallization is possible in a narrow temperature interval of 5–7° near the crystallization temperature. The effect of the directed crystallization on the magnetic properties is evident from a giant increase in coercivity, up to 1000 times. The directed crystallization was also assisted by application of a magnetic field which resulted in greater increase in coercivity, up to 1500 times and the coercivity value reached 69400 A m^{-1}. For comparison, at a standard crystallization the coercivity increases by 8–10 times being in the range of 2000–4000 A m^{-1}. The developed micro-magnets can find a range of applications in miniature sensors, actuators, and manipulators.

1 Introduction Micron sized magnetic poles which produce spatial distribution of magnetic fields at a micron scale are required for a large number of applications including the manipulation of biological objects [1], biasing of microsensors and actuators [2], and diamagnetic levitation [3]. In bio-analytical and biomedical systems, it is often required to move and position small particles, cells, and molecules. In order to handle such objects at the micro scale, many magnetic devices have been developed. If soft magnetic elements are used [4–6], an external source of magnetic field is needed to polarize them. Microelectromagnets [7–9] are controlled with a power supply. This may not be desirable for practical use.

A system of permanent micro magnets (μ-magnets) [10] provides passive contactless manipulation, trapping, and arraying of particles and micro-droplets in a required way. Micro magnets can be produced from individually micromachined bulk SmCo or NdFeB magnets. However, this method is hardly compatible with the design of guidance system of complex shapes. Many techniques for obtaining μ-magnets are being developed, such as thermomagnetic patterning [11], however, each suffers from some limitations. The technology for cheap, easy, and fast integration of good quality μ-magnets is still to be established. In this work, we propose a novel method of μ-magnet fabrication from amorphous glass-coated magnetic microwires undergone directed crystallization.

Magnetic glass-coated microwires in amorphous or nanocrystalline state [12, 13] are attractive for technology miniaturization as they exhibit a number of outstanding effects. This includes the magnetoimpedance effect [14, 15] and magnetic bistability [16] used in high-performance sensors, the microwave properties useful for absorption materials [15], the shape memory and magnetocaloric effects [17, 18] for magneto-mechanical actuators, magnetocaloric devices, and magnetic refrigeration. In all these applications, combining the functional wire with the hard magnetic wire serving as a micromagnet can provide additional tuning.

The wires are produced by modified Taylor–Ulitovsky method [19, 20] based on drawing the glass-metal composite and fast solidification. This technique allows a strict control of geometry with the metallic core diameter varying between 1–30 μm and the glass coating thickness in the range of 0.5–20 μm. The wire shape and dimensions are also suitable for embedding them in fiber reinforced composites [15] to introduce electromagnetic functionality.

Crystallization processes play an important role in determining the wire magnetic properties. The methods that control the crystal nucleation and growth are of great interest to tailor these properties. A process of crystal gross of a certain shape in a given direction and at a constant speed is known as directed crystallization. There are a number of methods to realize the directed crystallization, which includes the Bridgman–Stockbarger method, Chokhralskiy method, zone melting (vertical and horizontal), etc. [21, 22]. Recently the effect of templates is used for directional crystallization. In this work, a directed crystallization from amorphous state is realized by moving the thermally activated crystallization front along the glass-coated magnetic microwires of Co-rich composition. The directed crystallization was also assisted by the application of a magnetic field. The efficiency of the process was confirmed by giant increase in the coercivity.

The transition from an amorphous metastable state into a stable crystalline state occurs when increasing the temperature above the critical value through a number of metastable phases. Thermally activated processes of structural relaxation, diffusion, and local crystallization are responsible for the formation of certain phases. Changing the temperature regimes makes it possible to control the extent of crystallization. In particular, soft magnetic alloy systems Fe–Si–B with addition of Cu and Nb known as Finemet are produced by partial crystallization of a corresponding amorphous matrix [23–25]. They have a nanocrystalline structure with ferromagnetic crystallites of a size 10–30 nm distributed in the amorphous matrix, which occupies 20–40% of the total volume. These alloys possess a record low coercivity and high permeability. In this work, our target is to realize hard magnetic alloys using the controlled crystallization from an amorphous state.

It is known that the coercivity of the magnetization loop increases greatly at crystallization. The directed crystallization resulted in a giant increase in coercivity up to 1000 times and up to 1500 times in the presence of a magnetic field.

2 Experimental Crystallization of an amorphous solid is a complex process involving simultaneous nucleation and growth of crystallites. Firstly, an increase in energy is required to form a new surface surrounding a crystallite. The energy is usually supplied in the form of thermal energy by increasing the temperature of the material. An amorphous state is metastable so upon crystallization a release of energy occurs, which can be used for maintaining the process in a controlled way.

The directed crystallization is typically considered for metals and alloys from liquid to solid state in the direction of the temperature gradient and thermal flux. Here the directed crystallization is realized from amorphous state. Glass-coated amorphous microwires of the composition $Fe_{4.3}Co_{67.7}Si_{11}B_{14}Cr_3$ with the total diameter of 29 μm and the metal core diameter of 25 μm were used.

The structural state of the microwires (amorphous or crystalline) was investigated by XRD with Cu K_α radiation. The crystallization temperature range was examined by using the differential scanning calorimeter (DSC) at a heating rate of 0.33 $K\,s^{-1}$. It is known that the coercivity strongly increases at crystallization so the change in coercivity may be used as an additional indicator of a crystalline state.

The heating requirement for the directional crystallization is a positive temperature gradient at the crystallization front in order to avoid the concentration overcooling, crystallite nucleation in the metastable phase volume, and instability of the crystallization front. A specially designed oven was used to ensure proper heat conditions. The central portion of a long tube oven had a nearly uniform temperature distribution as shown in Fig. 1. The constant temperature is maintained with the help of smaller heating coils of 70 mm long placed at the both ends. As a result, the temperature variation in the central part was less than 2°. The oven temperature could be increased up to 570 °C. This is sufficient to realize the primary crystallization conditions. A coil mounted on a quartz tube and located at the end of the operational zone provided local overheating. The rate of temperature variation with time was no more than 1° per minute.

The wire sample was placed in the middle portion of the oven with uniform temperature (about 100 mm long). For directed crystallization, the wire is heated to the temperature slightly below the primary crystallization temperature. The crystallization process was initiated by local overheating and releasing the latent heat of the transition on the phase boundary, after which the crystallization propagated over the entire wire. These temperatures should be carefully chosen so the phase transition heat would be sufficient to support the crystallization propagation. Thus, in the

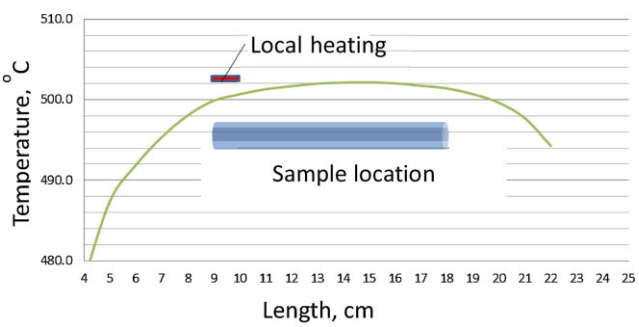

Figure 1 Temperature distribution along the tube oven used for directed crystallization process.

experiment, the phase boundary is created and the conditions for its propagation is realized.

The oven with the sample could be placed inside a solenoid of 250 mm long, which generated a dc magnetic field up to 1000 Oe along the tube. The temperature was controlled by thermocouples located along the oven.

The sample comprising 10–12 microwires was placed in the oven with a temperature about the primary crystallization temperature found from DSC curve for 5–7 min to reach the thermal equilibrium and then taken out for the coercivity measurements by a standard inductive method. In the amorphous state, the coercivity of FeCo wires is below 100 A m^{-1} and it increases several times in the crystalline state. Therefore, measuring the coercivity can be used for fast controlling the occurrence of the phase transition. The lowest annealing temperature at which the coercivity jump was observed was regarded as the onset crystallization temperature T_{cr}.

After defining T_{cr}, the temperature in the oven was set slightly below this value (by 5–7°) and the wire sample in an amorphous state was placed inside. The local heating was applied for 20–30 s to rapidly increase the temperature of the sample edge by additional 50–70°. This thermal flux originates the crystallization and its propagation along the wires. The optimal temperature of the local heating is found by measuring the coercivity along the wire sample.

The process of directed crystallization was also conducted in the presence of the magnetic field. After the sample's temperature was set slightly below T_{cr}, the solenoid and local heating were powered during 20–30 s. The oven temperature and the local heating temperature were the same as in the experiments without a magnetic field.

The hysteresis loops were measured by a vibrating sample magnetometer at quasi-dc condition. For this experiment, the wire was folded to form a sample of 9 mm long.

3 Results and discussion As-cast amorphous microwires have a bistable type of the hysteresis loop, as shown in Fig. 2, with a small coercivity in the range of 15–50 A m^{-1}. This magnetization behavior is consistent with an axial anisotropy which is induced by coupling between the tensile stress and positive magnetostriction. Although Co-alloys possess a negative magnetostriction, small additions of Fe or Mn change the sign of magnetostriction [26]. The temperature range for transition to the crystalline state is examined by the differential scanning calorimetry (DSC) as shown in Fig. 3 for exothermal process. It is seen that the crystallization proceeds in two stages and the heat release can be more efficient in the second stage. The primary crystallization temperature is about 510 °C. The crystallization conditions depend on many factors, such as alloy concentration, mechanical stresses, and physical size of the samples. Thus, for alloys (FeCo)SiB when the concentration of boron increases from 8 to 12 at.% the crystallization

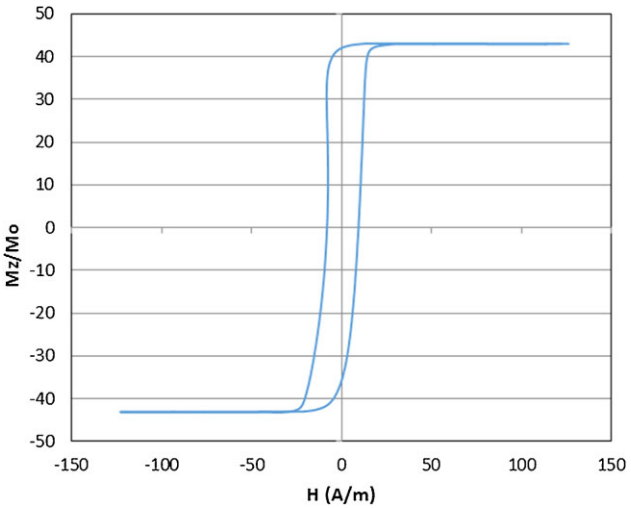

Figure 2 Magnetization curves of as-cast glass-coated amorphous microwires of the composition $Fe_{4.3}Co_{67.7}Si_{11}B_{14}Cr_3$.

temperature may increase from 455 to 530 °C. The obtained value of T_{cr} is consistent with previous studies of similar alloys [27–29]. The Curie temperature in the amorphous state is smaller than T_{cr} and is found to be 360 °C. Therefore, in the temperature range before crystallization the wire is in a paramagnetic state. The Curie temperature of the crystalline phases is larger than T_{cr} so upon crystallization the magnetic state is restored.

Usual crystallization when the wire sample is heated at a temperature above 550 for 10 min resulted in increase in coercivity up to 100 times so the coercivity of crystallized samples was 2000–5000 A m^{-1}. This is expected as the soft magnetic properties typical of amorphous alloys deteriorate at crystallization which typically produces the formation of rather coarse microstructure with the grain size of about 0.1–1 μm.

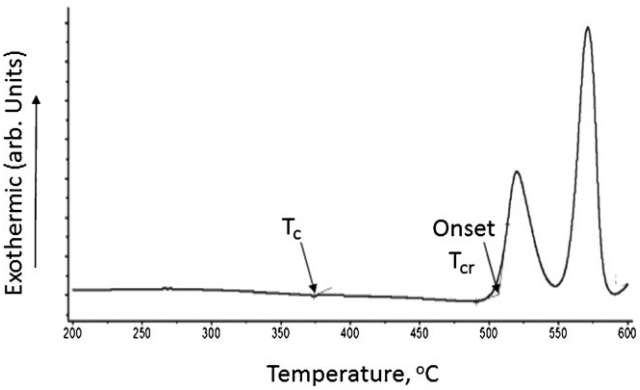

Figure 3 DSC exothermic curves of glass-coated microwires of the composition $Fe_{4.3}Co_{67.7}Si_{11}B_{14}Cr_3$ heated from amorphous state at the rate of 0.33 K s^{-1}.

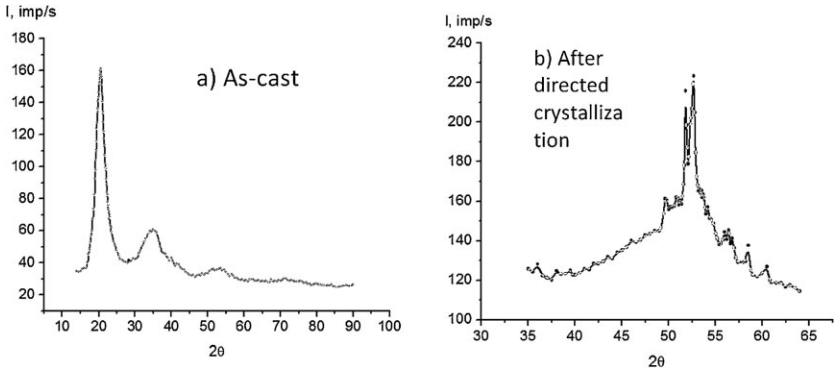

Figure 4 X-ray diffraction patterns of the $Fe_{4.3}Co_{67.7}Si_{11}B_{14}Cr_3$ alloy microwire: in (a) as-quenched state and in (b) after directed crystallization.

The DSC curve shown in Fig. 3 does not reveal a super-cooled liquid state and the directed crystallization from a solid amorphous state is not easily expected. However, the presence of a tensile stress may increase the crystal growth rate and promote the crystallization in this direction [30, 31]. The process of directed crystallization was confirmed by the XRD patterns given in Fig. 4. The amorphous state of as-cast microwire produces a single broad diffraction peak (Fig. 4a). After directed crystallization the hexagonal α-Co phase is formed and also borides of Co_3B and Si_3B represented by smaller peaks. The background corresponds to the residual amorphous matrix. These XRD patterns are consistent with the results reported in Refs. [27, 28] for CoSiB alloys annealed at 500–550 °C. Similar XRD patterns are obtained for wires undergone directed crystallization under the effect of a magnetic field.

The microstructure was further investigated by electron microscopy of the longitudinal shear (Fig. 5a) of the microwire after directed crystallization in the presence of the magnetic field. The shearing was done by argon ion beam in the microscope column. The application of the ion beam cuts out some of the amorphous matrix. It is seen that the crystallites have a dendrite shape and their axes are oriented mainly along the wire axis, that is, along the propagation of the crystallization front.

Figure 6 shows the hysteresis curves of the wires undergone the directed crystallization. The magnetizing field was applied along the wire and perpendicular to the wire. For the longitudinal magnetization, the loops are close to rectangular shape with the coercivity of 28000 A m^{-1} and the ratio of remanence to saturation is about 73%. In the perpendicular direction, the magnetization nearly linearly increases with the field.

Figure 7 shows the hysteresis curves of the wires subjected to field-assisted directed crystallization. The wires of different length were used for measurements. In average, the coercivity was 36000 A m^{-1}, which is higher than in the case of samples undergone the directed crystallization without a magnetic field. For shorter wires, the remanence-to-saturation ratio could be almost 90% and the loops have more pronounced bistable behavior. However, as the longer

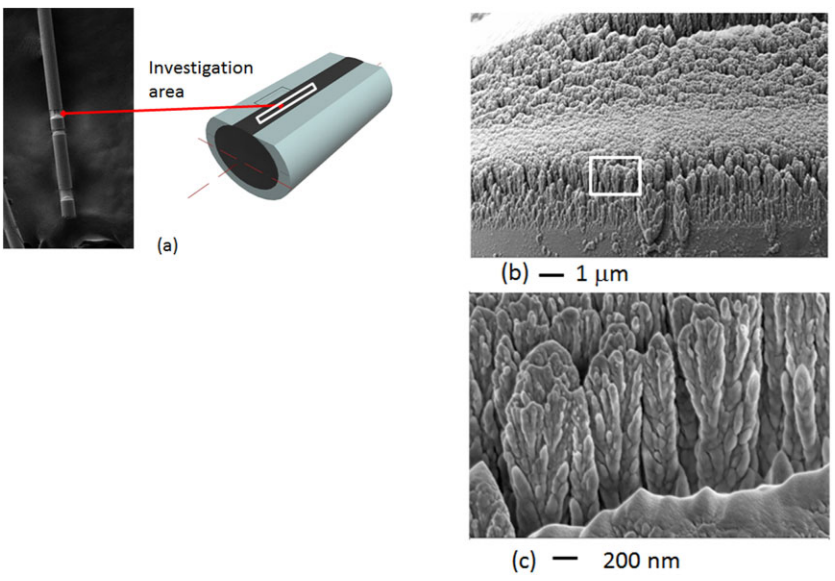

Figure 5 Electron microscopy of a longitudinal shear of the microwire undergone directed crystallization in the presence of a magnetic field. In (a), the position of the investigated shear is shown. In (b) and (c), the image of the highlighted area is shown with different magnification.

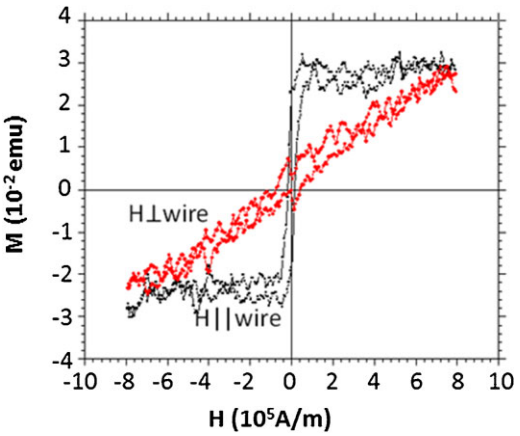

Figure 6 Hysteresis loops of $Fe_{4.3}Co_{67.7}Si_{11}B_{14}Cr_3$ wires after directed crystallization measured in a magnetic field along the wire and perpendicular to the wire. The wire length was 9 cm and it was folded to fit the area of $9 \times 9\,mm^2$. The longitudinal coercivity is $28000\,A\,m^{-1}$ and the ratio of remanence to saturation is about 73%.

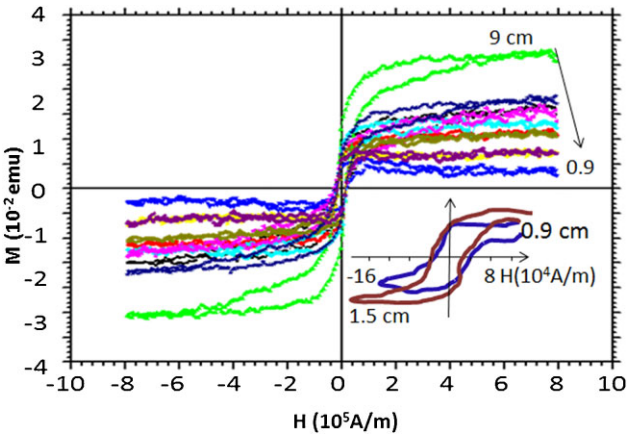

Figure 7 Hysteresis loops of $Fe_{4.3}Co_{67.7}Si_{11}B_{14}Cr_3$ wires after directed crystallization assisted by the magnetic field, for different wire length from 0.9 to 9 cm. The decrease in length is designated by the arrow. The magnetizing field is along the wire. The coercivity is about $36000\,A\,m^{-1}$. Insert shows the hysteresis behavior at smaller fields for wires of length 15 and 9 mm.

wires were folded, the decrease in remanence is not specifically the effect of length.

The increase in the coercivity in the samples after directed crystallization can be explained as follows. It is known that microstructure is greatly responsible for the magnetic coercivity. Thus, the decrease in grain size down to the domain wall scale increases the coercivity up to a value dictated by the anisotropies and magnetization. The directed crystallization could result in such microstructure.

The other mechanism of enhanced coercivity may be related with a change in elastic and magnetoelastic energies. The heat treatment of amorphous alloys below the crystallization temperatures relaxes residual internal stresses, but some stress remains especially the stress caused by the metal–glass interface. The solid-phase transformation of a metastable amorphous material into a crystal starts with nucleation releasing the excess of energy which contributes to the strain energy in the amorphous matrix as well as in the crystallites [30]. The highest strain-energy density region is at the interface of stable/metastable phases which propagates along the wire forming additional magnetoelastic pinning sites for magnetic domain walls. The presence of a magnetic field may change the spatial distribution of the magnetoelastic energy.

The Curie temperature of the crystalline alloy is considerably higher than the crystallization temperature, so the field effect on the coercivity could be explained by the field-induced anisotropy upon crystallization due to, for example, directional pair ordering of Fe and Co atoms [32, 33]. However, the applied field was below 0.1 T while the field-induced anisotropy requires much larger fields in the order of 1–2 T. Also, in our case, the magnetic field was applied during a short time. Therefore, the field-induced anisotropy is unlikely responsible for the observed effects.

The directed crystallization was realized in a number of samples with slightly different conditions and large deviation in the coercivity was observed. The presented results correspond to averaged data. The range of coercivities is given in Table 1. It is seen that the coercivity up to $69400\,A\,m^{-1}$ could be achieved by magnetic field assisted directed crystallization.

Table 1 Range of coercivity variations in microwires with different microstructure.

annealing treatment of microwire of the composition $Fe_{4.3}Co_{67.7}Si_{11}B_{14}Cr_3$	coercitivity ($A\,m^{-1}$)		
	min.	max.	average
initial amorphous wire	20	50	30
undergone usual crystallization at a temperature of 565 °C	2000	4300	3150
undergone directed crystallization at a temperature of 510–515 °C with local temperature increment of 50–70 °C	16000	46700	31350
undergone directed crystallization with a magnetic field	25500	69400	47450

4 Conclusions Directed crystallization of amorphous glass coated microwires of Co-rich composition was realized with the aim to obtain micron-sized permanent magnets. The increase in coercivity from $20\,A\,m^{-1}$ in amorphous state up to $69400\,A\,m^{-1}$ was obtained when the crystallization front propagation starts in the presence of a magnetic field of magnitude below 1 kOe. The precise nature of the giant increase in the coercivity requires further investigations. Such micro-magnets can find a range of applications in miniature sensors, actuators, and manipulators.

Acknowledgement L. V. Panina acknowledges the support for this work under Russian Federation State Contract for organizing a scientific work.

References

[1] M. A. M. Gijs, F. Lacharne, and U. Lehmann, Chem. Rev. **110**, 1518 (2010).
[2] V. Neu, A. Anane, S. Wirth, P. Xiong, S. A. Shaheen, and F. J. Cadieu, J. Appl. Phys. **87**, 5350 (2000).
[3] P. Kauffmann, A. Ito, D. O'Brien, V. Gaude, F. Boue, S. Combe, F. Bruckert, B. Schaack, N. M. Dempsey, V. Haguet, and G. Reyne, Lab Chip **11**, 3153 (2011).
[4] M. Shikida, A. Ito, and H. Honda, Lab Chip **8**, 134 (2008).
[5] P. Tseng, D. Di Carlo, and J. W. Judy, Nano Lett. **8**, 3053 (2009).
[6] T. Henighan, A. Chen, G. Vieira, A. J. Hauser, F. Y. Yang, J. J. Chalmers, and R. Sooryakumar, J. Biophys. **98**, 412 (2010).
[7] H. T. Huang, C.-Y. Chen, and M.-F. Lai, J. Appl. Phys. **109**, 07B315 (2011).
[8] H. Lee, A. M. Purdon, and R. M. Westervelt, IEEE Trans. Magn. **40**, 2991 (2004).
[9] Q. Ramadan, D. Poenar, and C. Yu., Microfluid Nanofluid **6**, 53 (2009).
[10] K. Hoshino, Y.-Y. Huang, N. Lane, M. Huebschman, J. W. Uhr, E. P. Frenkel, and X. Zhang, Lab Chip **11**, 3449 (2011).
[11] F. Dumas-Bouchiat, L. F. Zanini, M. Kustov, N. M. Dempsey, R. Grechishkin, K. Hasselbach, J. C. Orlianges, C. Champeaux, A. Catherinot, and D. Givord, Appl. Phys. Lett. **96**, 102511 (2010).
[12] M. Vazquez (ed.), Magnetic Nano- and Microwires (Woodhead Publishing, Elsevier Ltd., Oxford, 2015).
[13] M. Vazquez, H. Chiriac, A. Zhukov, L. Panina, and T. Uchiyama, Phys. Status Solidi A **207**, 1 (2010).
[14] L. V. Panina, Phys. Status Solidi A **206**, 656 (2009).
[15] F. Qin and H.-X. Hua-Xin, Prog. Mater. Sci. **58**, 183 (2013).
[16] J. Olivera, R. Varga, V. M. Prida, B. Hernando, and A. Zhukov, Phys. Rev. B **82**, 094414 (2010).
[17] M. Ilyn, V. Zhukova, J. D. Santos, and A. Zhukov, Phys. Status Solidi A **205**, 1378 (2008).
[18] V. Vega, L. González, J. García, W. O. Rosa, D. Serantes, V. M. Prida, G. Badini, R. Varga, J. J. Sunol, and B. Hernando, J. Appl. Phys. **112**, 033905 (2012).
[19] H. Chiriac and T. A. Ovari, Progr. Mater. Sci. **40**, 333 (1997).
[20] V. S. Larin, A. V. Torcunov, A. Zhukov, J. Gonzalez, M. Vazquez, and L. Panina, J. Magn. Magn. Mater. **249**, 39 (2002).
[21] A. A. Chernov, Modern Crystallography III: Crystal Growth (Springer, Berlin, Heidelberg, New York, 1984).
[22] M. S. Kouznetsov, I. S. Lisitsky, S. I. Zatoloka, and V. V. Gostilo, Nucl. Instrum. Methods A **531**, 174 (2004).
[23] G. Herser, Handbook of Magnetic Materials, Vol. 10 (Elsevier Science, Amsterdam, 1997), chap. 3.
[24] A. I. Gusev and A. A. Rempel, Nanocrystalline Materials (Cambridge International Science Publishing, Cambridge, 2004), p. 351.
[25] A. L. Adenot-Engelvin, C. Dudek, F. Bertin, and O. Acher, J. Magn. Magn. Mater. **316**, e831 (2007).
[26] A. Zhukov and V. Zhukova, Magnetic Properties and Applications of Ferromagnetic Mircowires with Amorphous and Nanocrystalline Structure (Nova Science Publishers, Inc., New York 2009), p. 68.
[27] R. Nowosielski, A. Zajdel, S. Lesz, B. Kostrubiec, and Z. Stoklosa, J. Achiev. Mater. Manufact. Eng. **27**, 147 (2008).
[28] S. Lesz, R. Nowosielski, B. Kostrubiec, and Z. Stoklosa, J. Achiev. Mater. Manufact. Eng. **16**, 35 (2006).
[29] M. Spilka, S. Griner, and A. Kania, Archiv. Mater. Sci. Eng. **56**, 61 (2012).
[30] J. Malek, Thermochim. Acta **355**, 239 (2000).
[31] D. N. Lee, J. Phys. Chem. Solids **72**, 1330 (2011).
[32] K. Suzuki, N. Ito, J. S. Garitaonandia, J. D. Cashion, and G. Herzer, J. Non-Cryst. Solids **354**, 5089 (2008).
[33] P. R. Ohodnicki, J. Long, D. E. Laughlin, M. E. McHenry, V. Keylin, and J. Huth, J. Appl. Phys. **104**, 113909 (2008).